

## Hydrothermal Alteration Mapping for Geothermal Exploration in Manda-Inakir Area, NW of the Republic of Djibouti

Ahmed, A.

Office Djiboutien de Développement de l'Energie Géothermique (ODDEG), route d'Arta PK 20, Djibouti

araksan\_ahmed@yahoo.fr

**Keywords:** Geothermal, Manda-Inakir, Hydrothermal alterations, Remote sensing, Landsat 8 OLI, False Color Composite (FCC), Band ratio (BR), Combination of Band ratio.

### ABSTRACT

Adopted in different domains, remote sensing is the science of obtaining information about an area through analyzing data collected by a device or a sensor without direct contact with the object under investigation. In a geothermal survey, this technique can be useful during the prefeasibility stages of exploration. The area of this study is located in the Afar depression in East Africa. This depression is the result of a triple junction of three rifts: the continental East African Rift, the Gulf of Aden, and the Red sea oceanic Rifts (Vellutini, 1990). Among the geological characteristic structures of Afar depression, the Manda-Inakir axial zone will be the center of this research. Situated in NW part of the Republic of Djibouti, it extends ENE-WSW across the boundary with Ethiopia. This is a predominantly basaltic unit and strongly fractured in NW-SE direction. Based on the last geothermal prospect of the Republic of Djibouti in 2014, the area is considered as a potential geothermal resource area for the country. Despite the lack of geophysical or geochemical data, this paper aims to map hydrothermal alterations of the Manda-Inakir area by using remote sensing to provide the basis for future geothermal investigations. A Landsat 8 OLI image of this site has been used. Preprocessing was the first step by carrying out an atmospheric correction (FLAASH) with Envi 5.3 software. Then the False Color Composite (FCC), Band ratio (BR) and a Combination of Band ratio methods have been applied for distinguishing the hydrothermal alteration. The different maps have been edited with ArcMap software. Finally, the resulted maps show the presence of hydrothermal alteration minerals in several zones in Manda-Inakir field that could become targets for further geothermal exploration.

### 1. INTRODUCTION

In the last two decades, the technology of spectral remote sensing has improved significantly (Sabins, 1999). Indeed, using remote sensing imagery data has become a helpful tool, which provides different information such as lithology, vegetation, thermal anomalies, lineaments, hydrothermal altered rocks, etc., based on the earth's surface composition and the rock's absorption of energy (Frutoso, 2015).

Besides, remote sensing techniques are economically attractive. Valuable information of a study area is obtained without direct contact with the object considered. After application for a long-time in mineral exploration, these methods have also been adopted in geothermal exploration. Knowing that water rock interaction in hydrothermal process produce various hydrothermal alteration minerals with spectral signatures, remote sensing data can be useful to create maps of altered areas associated with geothermal activity. Thus, these methods have been undertaken in this project.

In this paper, the Manda-Inakir area has been studied through processing Landsat 8 OLI image analysis. This rift-in-rift structure is located in the Afar Depression precisely in the northwest part of the Republic of Djibouti. This potential geothermal site is unfortunately not well known. The purpose of this preliminary study is to identify hydrothermal alteration zones to define new targets for future field explorations.

### 2. GEOLOGY OF MANDA-INKIR FIELD

The area of study is located in the northwest part of the Republic of Djibouti and crosses the border with Ethiopia. It corresponds to one of the "rift-in-rift" structures of the Afar Depression. There are two main rift zones observed in Djibouti, which are the Asal and Manda-Inakir axial series. Less studied than the Asal Rift, the Manda-Inakir range (Figure 1) is situated in a transitional zone between the intensively faulted "stratoid series" of central Afar Depression and the less fractured area along the red sea, the Danakil horst (Vellutini, 1989). Within this transitional zone, the Manda-Inakir range is linked to the Asal range by the Mak'Arassou transverse structure that is a NS left strip fault zone (Tapponier and Varet, 1974).

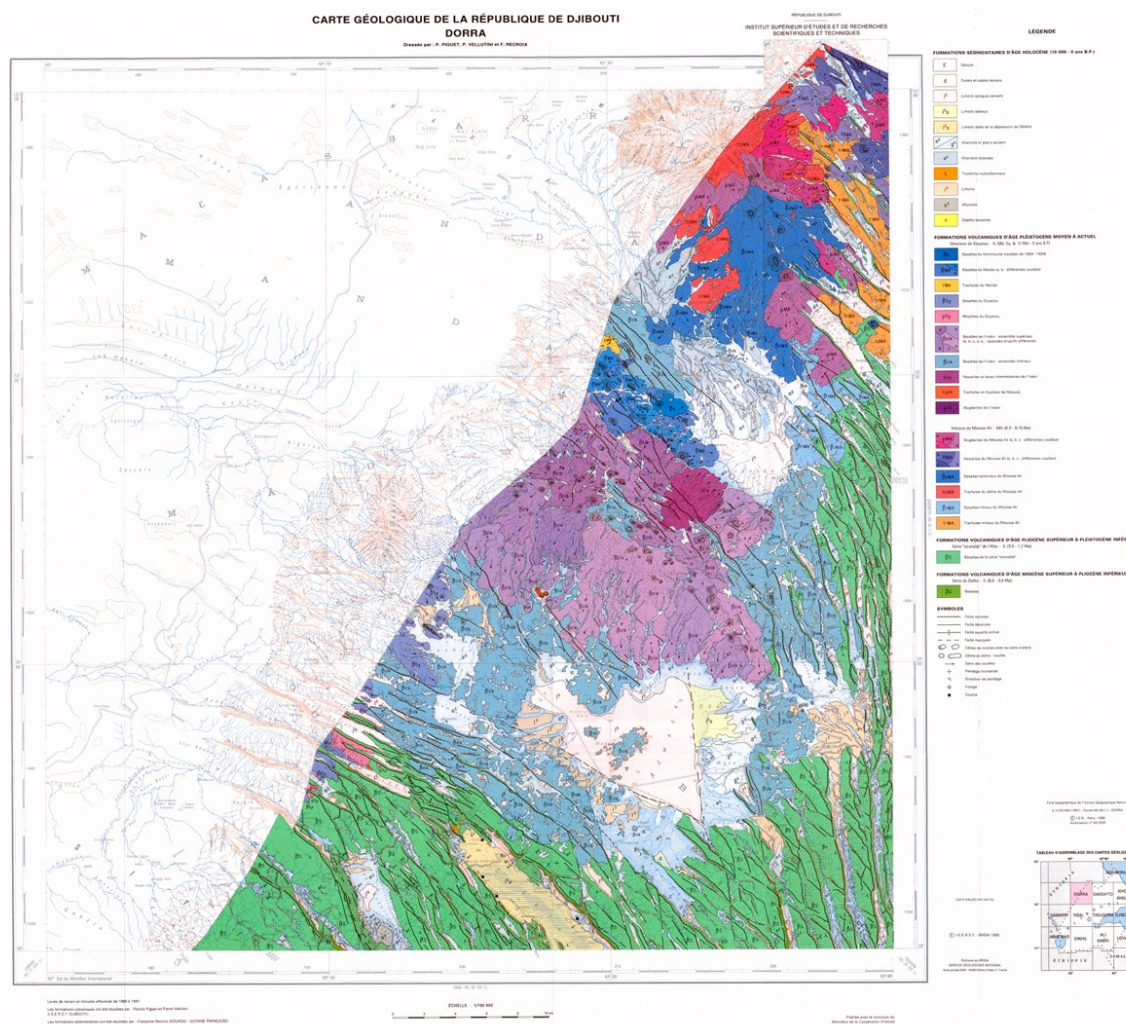


Figure 1: Geological map of Dorra in Manda-Inakir range formations in pale blue and purple (Piguet et al., 1995)

The Manda-Inakir field is divided into two rifting zones of different ages. The older, Inakir rift, aged 0,5-0,4 Ma, is located to the north of Dorra's plain (Civetta et al, 1975). Volcanic rocks overlying the basement of stratoid basalt in a NW-SE elongated dome or embryonic shield volcano compose it. This size of the dome is 25 km long and 12 km large. It is cut by the axis of the rift, which is 2 to 3 km wide with a faulted floor along the main NW-SE direction. The intense tectonic activity of these fractures leads to the creation of a graben structure by the collapse of the axial rift around 250 m. Along the marginal faults, basaltic cinder cones have erupted lava flows from the fissural basalts to the last mugearitic flows and spatter cones on the upper part of the shield volcano. These products have spread down the SW slope of the range (Vellutini, 1989; De Fino et al, 1973).

Manda is the second part of the Manda-Inakir range and younger than Inakir. This active, seismically and volcanologically, axial rift is mostly located in Ethiopia with a main tectonic direction WNW-ESE. Its southern part is distinguished in Djibouti parallel to the previous range of Inakir with an NW-SE direction. This is a dominantly fissural basaltic rift, bigger than Inakir with 42 km long and 15 km large. This rift zone of 2 km wide is built on numerous fissures of NW-SE direction. More of the open fractures are 1-3 m wide and many kilometers long. These can become faults that lead to a 25 m vertical displacement, giving hammock-like structures (Vellutini, 1989; Audin et al., 1990).

Several surface manifestations such as gas vents, hot springs, and fumaroles occur. They are mainly observed in the faulted formations where the NW-SE open faults cross the N-S trending faults. In this dry climate, the meteoric water is concentrated in the recent volcanic formations and nearby sedimentary plains and quickly infiltrates through the open fractures (Haga et al., 2012)

### 3. DATA AND METHODS

#### 3.1 Remote sensing data

Available since February 2013, Landsat 8 Operational Land Imager (OLI) is the last of eight series of Landsat satellites. This product is operated by the National Aeronautics and Space Administration (NASA). This land remote sensing satellite carries two sensors. The first one, Operational Land Imager (OLI), has nine shortwave spectral bands over a 185 km swath whose bands 1 to 7, band 9 presents a 30 m spatial resolution and band 8 (or panchromatic) with a spatial resolution of 15 m. The Thermal Infrared (TIR) sensor collects data for two thermal infrared bands (10 and 11) with a 100 m resolution covering a 185 km swath (Frutuoso, 2015) (Table 1).

**Table 1: Landsat 8**

<b>Landsat 8 Operational Land Imager (OLI) and Thermal Infrared Sensor (TIRS)</b>		
<b>Bands</b>	<b>Wavelength (micrometers)</b>	<b>Ground Sampling Distance (meter per pixel)</b>
Band 1 – Coastal aerosol	0.43 - 0.45	30
Band 2 – Blue	0.45 - 0.51	30
Band 3 – Green	0.53 - 0.59	30
Band 4 – visible Red	0.64 - 0.67	30
Band 5 – Near Infrared (NIR)	0.85 - 0.88	30
Band 6 – SWIR 1	1.57 - 1.65	30
Band 7 – SWIR 2	2.11 - 2.29	30
Band 8 – Panchromatic	0.50 - 0.68	15
Band 9 – Cirrus	1.36 - 1.38	30
Band 10 – Thermal Infrared (TIRS) 1	10.60 - 11.19	100*30
Band 11 – Thermal Infrared (TIRS) 2	11.50 - 12.51	100*30
* TIRS bands are acquired at 100 meter resolution, but are resampled to 30 meter in delivered data product		

In this study, the bands 1 to 7 were used for the identification of the spectral signature of hydrothermal alteration minerals. The satellite image was downloaded from the website “earthexplorer.usgs.gov” owned by USGS website and the Earth Resources Observation and Science Center (EROS). The characteristics of this satellite image data were obtained on June 27<sup>th</sup>, 2019 with a low cloud coverage (2.53%). The image displayed in this paper is projected in UTM Zone 38N using the WGS-84 datum as showed in figure 2.

### **3.2 Method analysis**

#### **3.2.1 Preprocessing**

For purposes of hydrothermal alteration mapping, the most used bands are located in the visible, near-infrared (NIR) and shortwave infrared (SWIR) wavelength. The Pre- and post-processing of Landsat 8 OLI image of the target area have been carried out using the software ENVI version 5.3. The pre-processing step seeks to undertake a radiometric calibration to get a calibrated image of the site. Then, FLAASH or Fast Line of Sight Atmospheric Analysis of Spectral Hypercubes, is an atmospheric correction used to obtain the surface reflectance of the study area as the final product is essential for further analysis in this project.

#### **3.2.2 Image processing**

Image processing methods transform the multispectral satellite data into images that enhance geological features in contrast with the background. With the development of satellite technology, using these methods has become a useful tool to discriminate hydrothermally altered and unaltered rocks, essential in hydrothermal alteration mapping (Frutoso, 2015).

In this study, three methods have been utilized for purpose to delineate hydrothermal alteration minerals in the Manda-Inakir geothermal field. The first one is the Single Band combination. It is important to note that Landsat imagery is formed by greyscale images of different spectral bands. Three bands in three canals of red, green and blue create a colorful composite image (Frutoso, 2015). The true color image is the combination of three visual primary grey images, hereby using the bands 4, 3 and 2 (RGB) as shown in figure 2. With the obtained image, it is possible to describe the outcrop rocks in dark brown color and black for the young basalt of Manda-Inakir in the north-western part, the rare vegetation is in green color and the water in blue. The white color corresponds to the sedimentary deposit in the plains.

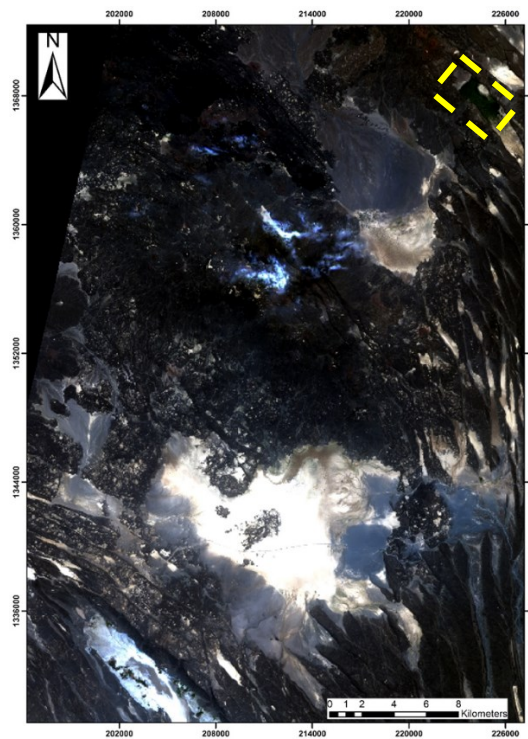


**Figure 2: True color composite (4, 3, 2) of Manda-Inakir field with rare vegetation in dark green (yellow box), water in blue and white for sedimentary deposit**

On the other hand, the combination of three bands in visible and infrared or only in infrared, in red, green and blue will provide a false color image that emphasis some characteristics of the selected spectral bands based on the spectral properties of the rocks and alteration minerals. Thus, different contrast-enhanced RGB combinations of SWIR, NIR and Visible were created for preliminary geological study (Frutuoso, 2015). The most contrasting band combination for lithological features and the first determination of probably altered area should include one visible (2, 3 or 4), one NIR (5) and one SWIR (6 or 7) band (USGS, 2015a; USGS, 2015c). The false color composite 5, 6, 7 (RGB) shows the exposed rocks in green and the vegetated areas in orange-brown. The light blue or cyan colored zones could be related to hydrothermal altered rocks (Figure 3).

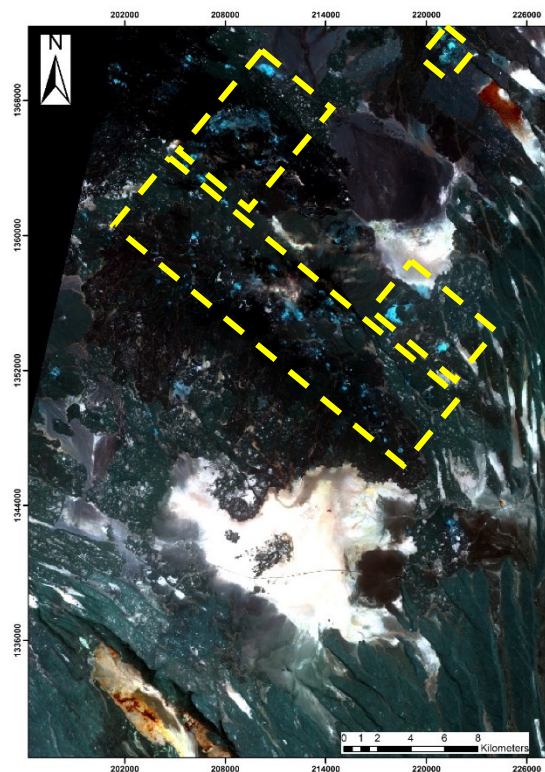


**Figure 3: False color composite 5, 6, 7 with exposed rocks in green, the vegetated areas in orange-brown and the light blue or cyan colored zones for hydrothermal altered rocks in yellow box**



Band ratio is the second technique carried out in this study. It is a method where one band of high reflectance is divided by another band of low reflectance (Goetz et al., 1975, Pour and Hashim., 2015). This technique improves the contrast and enhances compositional information while deleting useless details such as earth's surface, the shadow caused by topography surface and highlighting some features that cannot be observed with raw data (Sabins, 1997; Ali and Pour, 2014). Initially used for geological purposes and mining industry, several authors (Sabins, 1999; Rajesh, 2004; Han and Nelson, 2015; Mwaniki et al., 2015) presented different ratios listed as follow in figure 4: 4/2 iron oxide, 6/7 hydroxyl bearing rocks, 7/5 clay minerals, 6/5 ferrous minerals. The ratio 2/1 has been proposed by González (2018) for possible sulphur, anatase, covelite (Figure 5).

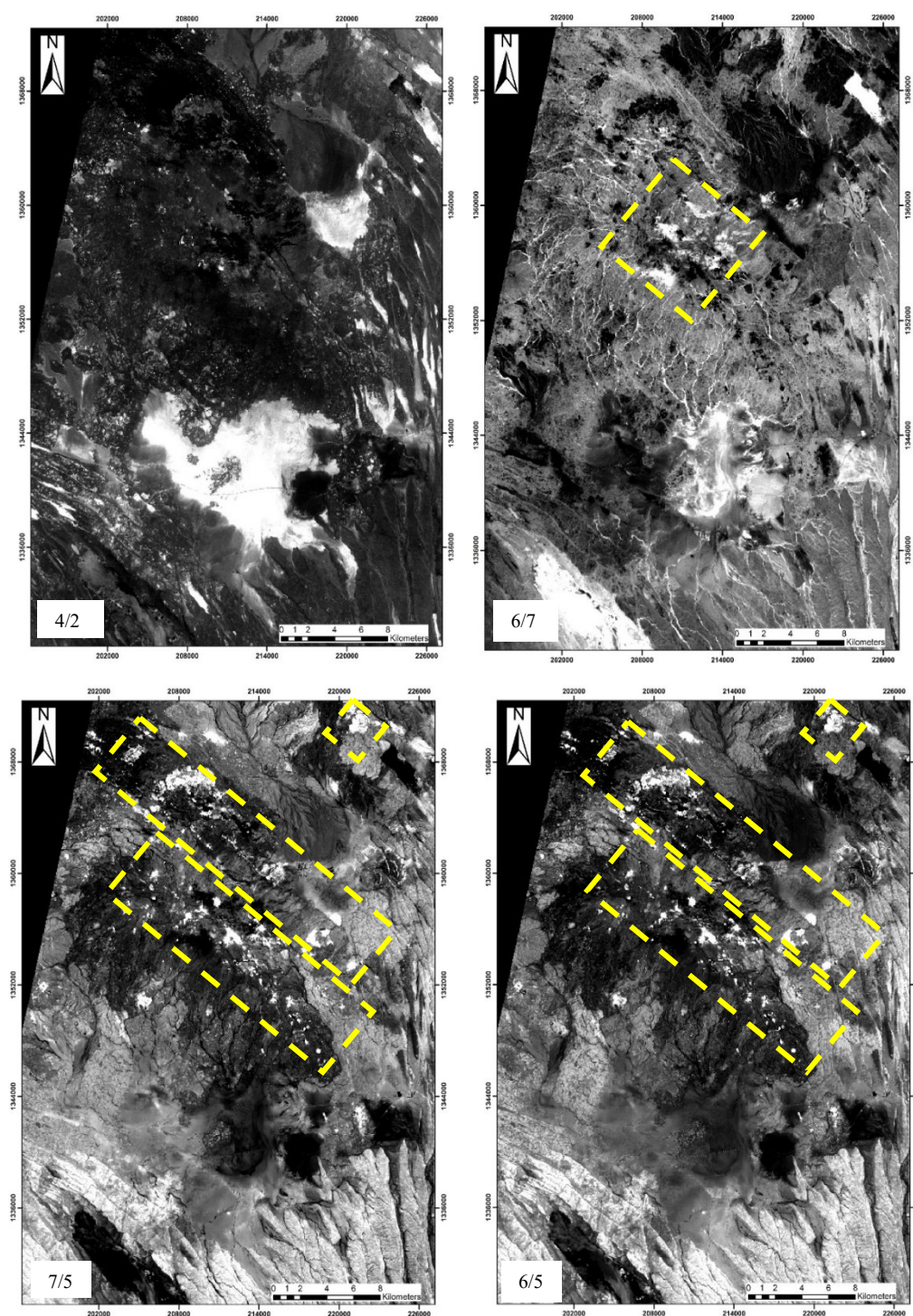


**Figure 4: Band ratios: 4/2 for iron oxide, 6/7 for hydroxyl bearing rocks, 7/5 for clay minerals, 6/5 for ferrous minerals. Alteration minerals deposition area in yellow box**

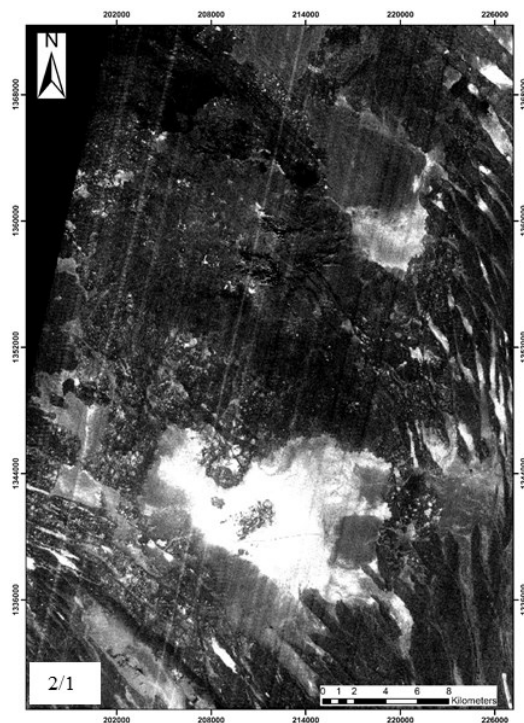


**Figure 5: Band ratio of 2/1 for sulphur, anatase, covelite by González (2018)**

These different band ratios can be combined to form a false color ratio composite, which is the third method. An image incorporating these band ratios will discriminate altered from unaltered ground and highlight areas where the concentration of these minerals occur (Rajesh, 2004). The advantage of the color ratio image is that it combines the distribution patterns of groups of minerals. However, the disadvantage is that the color patterns are not as distinct as in the individual ratio images (Sabins, 1999). Several combinations of ratios have been proposed.

Thus, Sabin (1999) and Ali and Pour (2014) have used the RGB of 4/2, 6/7 and 6/5 for lithological and hydrothermal alteration zones. The ratio 4/2 helps to highlight iron oxides areas as hematite, limonite, and jarosite with high reflectance in red color (Van der Meer, 2004). The ratio 6/7 enhances the clay minerals like kaolinite, illite, and montmorillonite. 6/5 shows the presence of ferrous minerals as goethite, hematite. Ali and Pour (2014) have also proposed a combination RGB of the bands 4/2, 6/7 and 5 to identify the lithology, the altered rocks, and vegetation. Kauffman's ration (7/5, 5/4, 6/7) is also used to separate vegetation from altered zones (Ali and Pour, 2014). The last combination of ratios used in this study has been presented by González (2018). The false color composite is formed by the bands 6/7, 6/5 and 2/1 (RGB). These results are presented in section 4 of this paper.

#### 4. RESULTS AND DISCUSSION

The false color composite of the bands 5, 6 and 7 shows the altered areas in cyan color (Figure 3). These hydrothermal altered areas appear in the Manda-Inakir formations and essentially along with the fractures of NW-SE direction. The question is to know which hydrothermal alteration is located in this zone.

The aim of creating different band ratios was to enhance the hydrothermal altered rocks and the associated minerals. Thus, five ratios of Landsat 8 OLI have been applied in this study to highlight different types of mineral alteration. The ratio of band 4 over band 2 (Figure 4) presents areas with abundant iron oxides in bright pixels. These areas are rare and disseminated in the geological outcrops and the bright regions correspond to the plains filled by sedimentary deposits. The ratio 6/5 discriminates ferrous minerals as goethite, hematite, in bright tone (Figure 4). Then the ratio 7/5 enhances the altered rocks with the presence of clays minerals (Figure 4). It appears that the hydrothermal altered areas shown by the false color composite (5, 6, 7) are highlighted in the grey-scale images of ratio 6/5 and 7/5. Clay minerals such as illite, kaolinite, and montmorillonite are highlighted in bright pixels by the ratio 6/7 (Figure 4). However, the pixels with high value located in the North-East and South-West part of the image are due to vegetation cover and sedimentary deposition. The last ratio of 2/1 (Figure 5) has been used by González (2018) suggesting the presence of Sulphur, anatase and covelite minerals in bright pixels. The results obtained from this ratio show that these alteration minerals deposits are rare. The brightest area corresponds to the silt formation in the plains. These results are summarized as below in the table 2.



**Table 2: Results of band ratio method**

Band ratios	Results
4/2	Abundant iron oxides in bright pixels
6/7	Clay minerals as illite, kaolinite, and montmorillonite in bright pixels
7/5	Altered rocks with the presence of clays minerals
6/5	Discriminates ferrous minerals as goethite, hematite, in bright tone
2/1	Presence of Sulphur, anatase and covelite minerals in bright pixels

For better highlighting results of the altered rocks, several false color composites have been utilized by combining the previous grey-scaled images. Kaufmann's ratio (7/5; 5/4; 6/7) (Figure 6a) has been tested to detect hydrothermal altered areas. The altered rocks are identified as bright orange. In this project, the altered rocks appear in dark violet by using Sabin's ratio (4/2; 6/7; 6/5) (Figure 6b).

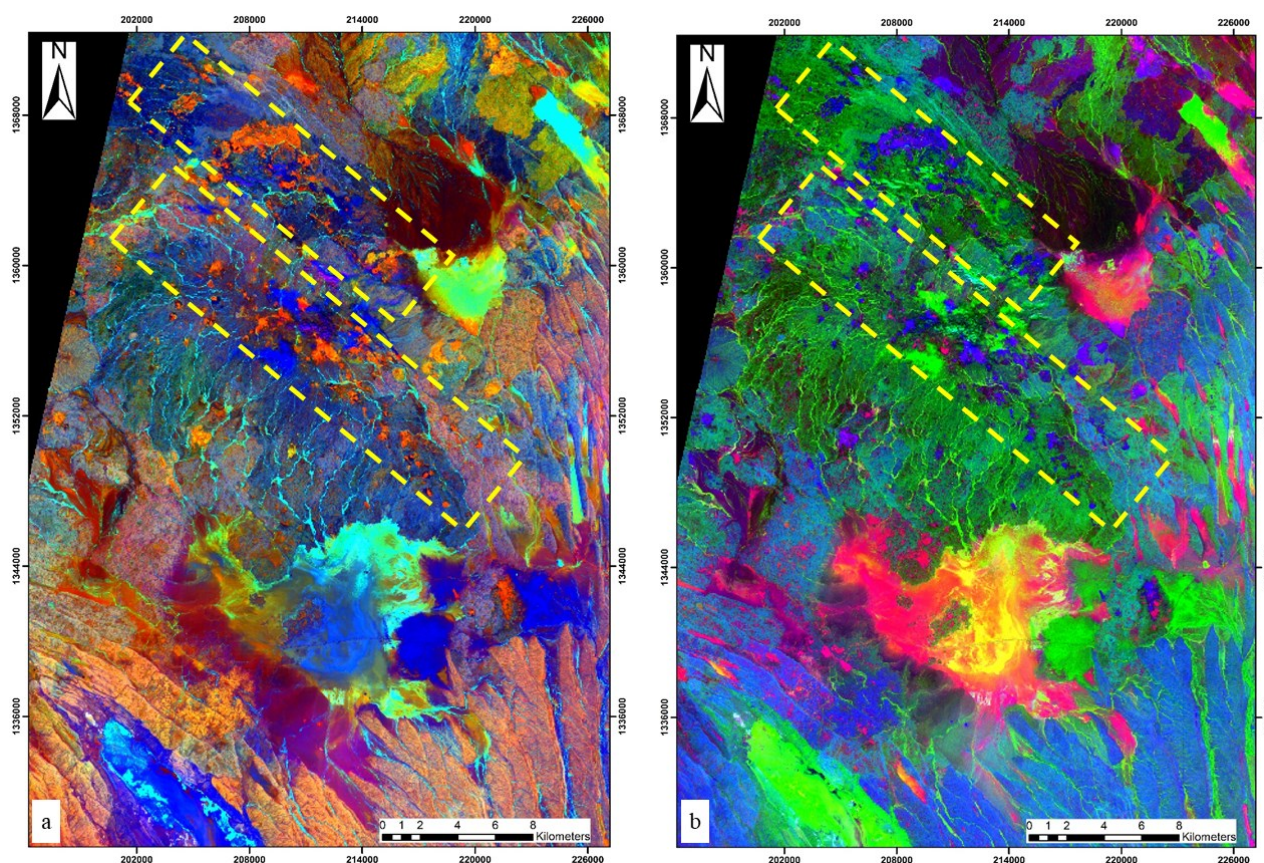


**Figure 6: (a) Kaufmann's ratio with altered rocks in bright orange; (b) Sabin's ratio with altered rocks in dark violet with alteration minerals deposition area in yellow box**

Then, the combination of 4/2, 6/7 and 5 seeks to highlight the hydrothermal alteration in dark magenta (Figure 7a). The last combination of ratios (6/7; 6/5; 2/1) has been used by González (2018). The alteration is presented as a strong green color. However, a yellow color is noticed mostly in the northwestern part of the map but also along with some fractures. It represents a high value of 6/7 and 6/5 ratio (González, 2018) as shown in figure 7b.



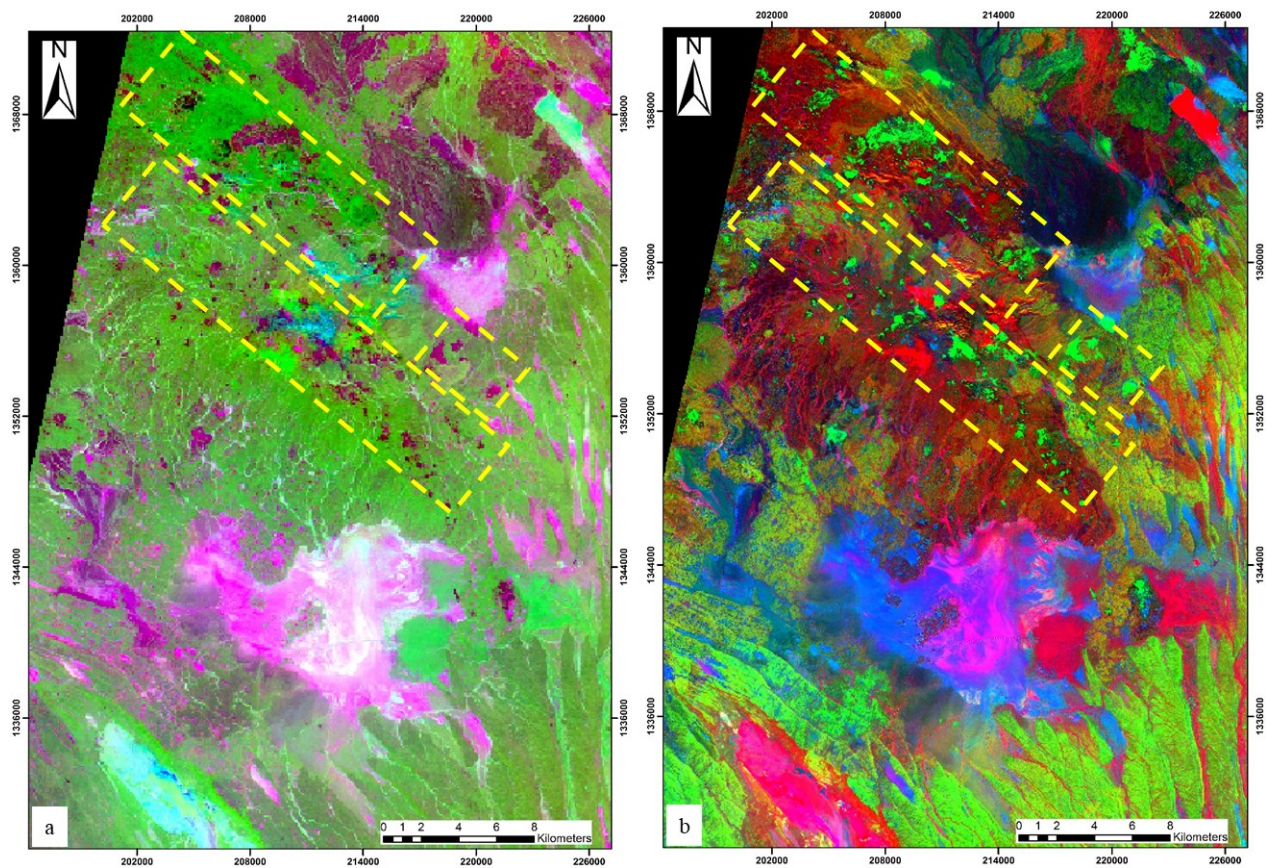


**Figure 7: (a) Pour and Hashim ratio with hydrothermal alteration in dark magenta; (b) Gonzalez ratio with alteration in strong green color with alteration minerals deposition area in yellow box**

According to the results of the data analysis, the alteration areas seem to be mainly located along with the fractures of the Manda-Inakir range in NW-SE direction. The hydrothermal alteration minerals could be related essentially to ferrous minerals and hydroxyl bearing rocks. Clay minerals surround them. However, these assumptions have to be verified by fieldwork exploration.

## 5. CONCLUSION

Remote sensing techniques are helpful in getting valuable data about a study area in the early stages of exploration. In this study, Manda-Inakir axial range, which is almost unknown but considered a potential geothermal field through its geological characteristics, has been chosen. By using remote sensing methods, through False Color Composite, Band ratios and a Combination of band ratios of Landsat 8 imagery, provided the very first overview of the hydrothermal alteration zones that could be found in the area. The hydrothermal alteration minerals are essentially found along with the major fractures in the NW-SE direction. Thus, the analysis of the results has led to maps that could be used to delineate specific zones for further geothermal exploration. In vast and unknown areas, it is recommended to use remote sensing methods as a tool in the early stage of geothermal project exploration to provide a first idea before site visit.

## REFERENCES

- Ali, A., & Pour, A. (2014). Lithological mapping and hydrothermal alteration using Landsat 8 data: a case study in ariab mining district, red sea hills, Sudan. *Int. J. Basic Appl. Sci*, 3., 199.
- Audin, J., Vellutini, P., Coulon, C., Piguet, P., & Vincent, J. (1989). The eruption of the Kammourta volcano (1928): an evidence of the present tectonomagmatic activity of the Manda Inakir range (Rep. of Djibuti). *Bull. Volcanol.*, 52, 551-561.
- Civetta, L., De Fino, M., Gasparini, P., Ghiara, M., & La Volpe, L. a. (1975). Structural meaning of central eastern Afar. *J. Geol.*, 83, 363-373.
- deFino, M., La Volpe, L., Lirer, L., & Varet, J. (1973). Geology and petrology of Manda-Inakir range and Moussa Alli volcano, central eastern Afar (Ethiopia and T.F.A.I.). *Rev. Geog. Phys. Géol. Dyn.*, (2) 15, 373-386.
- Frutuoso, R. M. (2015). *Mapping hydrothermal gold mineralization using Landsat 8 data. A case of study in Chaves license, Portugal.*
- Goetz, A. F., Rowan, L. C., & Kingston, M. (1982). Mineral identification from orbit: initial results from the Shuttle Multispectral Infrared Radiometer. *Science*, 218, 1020-1031.



- Haga, A. O., Youssouf, S. K., & Varet, J. (2012). The Manda-Inakir Geothermal Prospect Area, Djibouti Republic. *4th African Rift Geothermal Conference*. Nairobi, Kenya: MEERN.
- Han, T., & Nelson, J. (2015). Mapping hydrothermally altered rocks with Landsat 8 imagery : A case study in the KSM and Snow field zones , northwestern British Columbia. *Geological Fieldwork 2014, British Columbia Ministry of Energy and Mines, British Columbia Geological Survey Paper*, 103-112.
- Mwaniki, M. W., Moeller, M. S., & Schellmann, G. (2015). A comparison of Landsat 8 (OLI) and Landsat 7 (ETM+) in mapping geology and visualising lineaments: A case study of central region Kenya. *ISPRS - International Archives of the Photogrammetry, Remote Sensing and Spatial Information Sciences, XL-7/W3*, 897-903.
- Piguet, P., Vellutini, P., & Recroix, F. (1995). *Feuille ND-38-1-1 de Dorra à 1/100 000*. I.S.E.R.S.T.
- Pour, A., & Hashim, M. (2015). Hydrothermal alteration mapping from Landsat-8 data, Sar Chesmeh copper mining district, south-eastern Islamic Republic of Iran. *Journal of Taibah University for Science*, 9, 155-166.
- Ramírez-González, L. (2018). *Remote sensing of surface hydrothermal alteration, identification of minerals and thermal anomalies at Sveifluháls-Krýsuvík high-temperature geothermal field, SW Iceland*. Reykjavik: Háskólaprent.
- Sabins, F. (1999). Remote sensing for mineral exploration. *Ore Geol. Rev*, 14, 157-183.
- Tapponier, P., & Varet, J. (1974). La zone de Mak'arrasou en Afar : un équivalent émergé des « failles transformantes » océaniques. *C.R. Acad. Sci., D* 278, 317-329.
- USGS. (2015a). *Landsat 8 (L8) Data Users Handbook. Version*.
- USGS. (2015c, Accessed Aug.). *Frequently Asked Questions about the Landsat Missions*. Récupéré sur [http://landsat.usgs.gov/L8\\_band\\_combos.php](http://landsat.usgs.gov/L8_band_combos.php)
- USGS. Website, <https://earthexplorer.usgs.gov/>
- Van Der Meer, F. (2004). Analysis of spectral absorption features in hyperspectral imagery. *Int. J. Appl. Earth Obs. Geoinf*, 5, 55-68.
- Vellutini, P. (1990). The Manda-Inakir Rift, Republic of Djibouti: a comparison with the Asal Rift and its geodynamic interpretation. *Tectonophys.*, 172, 141-153.